

Heat Capacity and Other Properties of Body-Centered Cubic He<sup>4</sup>\*

D. O. EDWARDS AND R. C. PANDOLF

*Ohio State University, Columbus, Ohio*

(Received 29 November 1965)

The heat capacity at constant volume,  $C_v$ , of bcc He<sup>4</sup> has been measured for a number of molar volumes covering most of the bcc region of the phase diagram. The results can be represented to within 3% of  $C_v$  by a constant Debye  $\Theta$  of 16.95°K. Using the discontinuities in the heat capacity at the phase boundaries measured in this and in previous work, the compressibility  $\kappa$  is found to be  $(3.8 \pm 0.2) \times 10^{-3}$  atm<sup>-1</sup> and substantially independent of temperature, while values of the expansion coefficient  $\alpha$  found by the same method are between  $5 \times 10^{-3}$  and  $13 \times 10^{-3}$  deg<sup>-1</sup>. The values of  $\alpha$  are consistent with a Gruneisen equation with a Gruneisen constant  $\gamma \approx 2.6$ , the value found previously for hcp He<sup>4</sup>. The latent heats at constant volume at the lower and upper triple points  $T_1$  and  $T_2$  have been measured as a function of volume and give for the maximum entropy change at  $T_1$ , where (hcp+liq)  $\rightarrow$  (bcc), the value  $\Delta S_1/R = (9 \pm 1) \times 10^{-3}$ . The maximum entropy change at  $T_2$ , where bcc  $\rightarrow$  (hcp+liq), has the value  $\Delta S_2/R = (32 \pm 2) \times 10^{-3}$ . The triple-point temperatures were found to be  $T_1 = 1.463 \pm 0.002^\circ\text{K}$  and  $T_2 = 1.7715 \pm 0.001^\circ\text{K}$ . The intersection of the  $\lambda$  line with the bcc phase boundary has been confirmed to be  $\sim 10$  mdeg below the upper triple point. The entropy of the bcc phase at the transition line has been computed from the heat-capacity results and the latent-heat measurements, and is found to vary from  $S/R = 0.037 \pm 0.002$  at  $T_1$  to  $S/R = 0.068 \pm 0.003$  at  $T_2$ . The relation between  $S$  and  $C_v$  is the same as for the other low-pressure structures of solid He<sup>3</sup> and He<sup>4</sup>, indicating that the variation of  $\Theta$  with  $T$  and therefore the lattice spectra are similar. On the supposition that bcc He<sup>4</sup> is indeed like the other forms of solid helium, it is estimated that bcc He<sup>4</sup> would have a Debye  $\Theta$  at 0°K,  $\Theta_0$ , of 21°K for a molar volume of 21 cm<sup>3</sup>. This value of  $\Theta_0$ , when compared with the measured velocity of sound, indicates that bcc He<sup>4</sup> is elastically highly anisotropic, in agreement with the recent theory of Nosanow and Werthamer.

## I. INTRODUCTION

THE body-centered cubic (bcc) phase of He<sup>4</sup> was discovered, and its boundaries in the  $p$ - $T$  plane determined, by Vignos and Fairbank<sup>1</sup> during measurements of the velocity of longitudinal sound in solid helium. The structure of the phase was definitely established to be bcc by the x-ray work of Schuch and Mills,<sup>2</sup> and later Grilly and Mills<sup>3</sup> measured the molar volumes and pressure at melting and at the bcc-hcp transition (see Figs. 1 and 2). The bcc region of the phase diagram is only 0.04°K wide at constant pressure and not much wider at constant density, while the total variation of density across the phase is about 1%. The upper triple point  $T_2$  is very close to the  $\lambda$  curve of the liquid. The bcc structure is also found in solid He<sup>3</sup>, where it occupies a much larger area of the phase diagram, and its existence in both isotopes can be attributed to the dominant role played by the zero-point energy and the lattice entropy, both of which offset the higher potential energy in the bcc structure compared with the close packed structures.

Recently, the specific heat at constant volume of bcc He<sup>4</sup> has been measured by Ahlers<sup>4</sup> in a small range of the higher densities near to  $T_2$ . The lower densities were not measured because for these Ahlers was unable to form a block of solid helium in the filling tube of the calorimeter so as to keep the specimen at constant volume. His

results seem to indicate that bcc He<sup>4</sup> has remarkable properties: in particular that  $(\partial C_v / \partial V)_T$  is negative, implying a negative temperature coefficient of the thermal-expansion coefficient. By using his measurements of the discontinuities in  $C_v$  at the phase boundaries with the  $PVT$  data of Grilly and Mills, he was able to obtain negative values of the expansion coefficient itself.

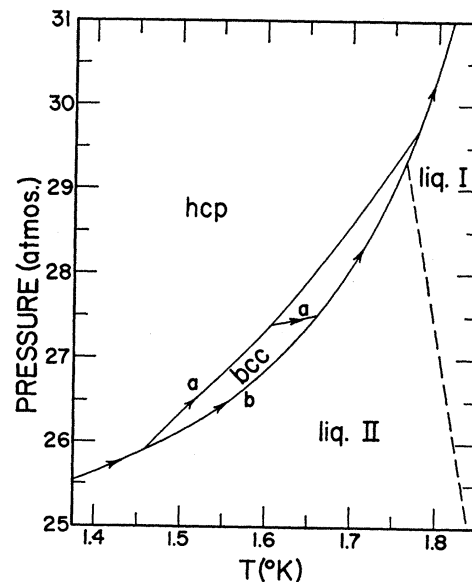


Fig. 1. Pressure-temperature diagram for He<sup>4</sup> in the neighborhood of the bcc phase. The phase boundaries have been drawn using the results of Grilly and Mills (see Ref. 3) with the temperatures corrected by Ahlers [see Eq. (3) and Ref. 4]. The arrows indicate two possible, constant-volume paths, a and b.

\* Work supported by the National Science Foundation and the U. S. Office of Naval Research.

<sup>1</sup> J. H. Vignos and H. A. Fairbank, Phys. Rev. Letters **6**, 265 (1961).

<sup>2</sup> A. F. Schuch and R. L. Mills, Phys. Rev. Letters **8**, 469 (1962).

<sup>3</sup> E. R. Grilly and R. L. Mills, Ann. Phys. (N. Y.) **18**, 250 (1962).

<sup>4</sup> G. Ahlers, Phys. Rev. Letters **10**, 439 (1963); Phys. Rev. **135**, A10 (1964).

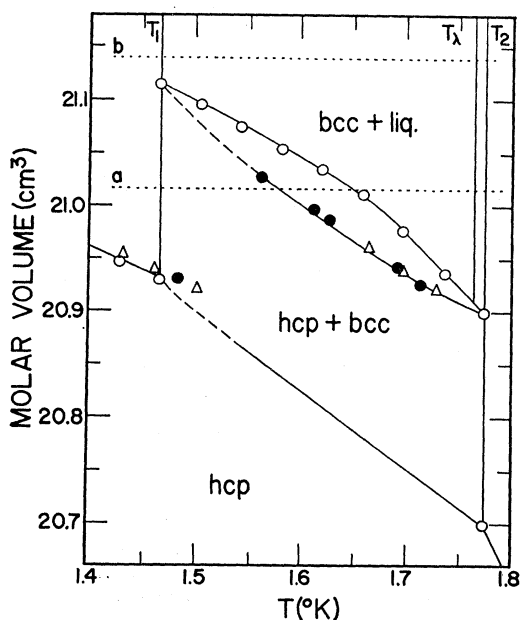


FIG. 2. Volume-temperature diagram for  $\text{He}^4$  in the neighborhood of the bcc phase. The open circles show the results of Grilly and Mills (see Ref. 3) with temperatures corrected with Eq. (3); the open triangles show the results of Ahlers (see Ref. 4) with volumes determined from bcc melting temperatures using Grilly and Mills' corrected bcc-(bcc+liq) melting line; the closed circles are the present results with volumes determined in the same manner, except for the point at 1.481°K where the volume was determined from the (hcp+bcc)-bcc boundary. The hcp-(hcp+bcc) line has been drawn using Grilly and Mills' data for  $\Delta V_{tr}$  and Ahlers' and the present results for the (hcp+bcc)-bcc line. The dashed lines a and b represent the constant-volume paths shown in Fig. 1.

In the present series of experiments no difficulty in blocking the capillary tube occurred, so that more or less the whole range of density has been covered. We have also been able to obtain measurements of the latent heats at the two triple points,  $T_1$  and  $T_2$ , as well as approximate values of the entropy and a small number of new points on the phase boundaries of the phase diagram.

The experimental apparatus and the techniques used in the present experiments have been described in our previous paper<sup>5</sup> on the heat capacity of hcp  $\text{He}^4$ , to which we refer the reader for details.

## II. RESULTS

### Measurements of the Temperature and Latent Heat at the Triple Points

As in our previous work<sup>5</sup> on hcp  $\text{He}^4$ , the heat capacity measurements were made at constant volume, so that samples with densities corresponding to the body-centered cubic region of the phase diagram followed a path like that labeled "a" in the molar volume-temperature diagram of Fig. 2 and in the  $p$ - $T$

diagram of Fig. 1. In some experiments specific-heat measurements were taken first in the single-phase hcp region and then in the two-phase, hcp+liquid region before the lower triple point temperature  $T_1$  was reached. At  $T_1$  it was invariably observed that some superheating of the hcp-liquid mixture occurred: The temperature of the calorimeter could usually be raised about 10 mdeg above  $T_1$  before the bcc phase finally appeared. The temperature then suddenly dropped and became more or less constant while the latent heat  $L_1$ , necessary to convert the sample to a hcp+bcc solid mixture was supplied by the heater. By measuring the "fore-drift" and "after-drift" before and after heating the calorimeter through  $T_1$ , it was possible to measure the latent heat to a few percent. The correction necessary for the heat supplied to raise the temperature of the sample and calorimeter was calculated from the heat-capacity measurements made above and below  $T_1$ . The principal difficulty in determining the latent heat like this was the very long time required to attain equilibrium in the two-solid hcp+bcc mixture. This was demonstrated when the heat was turned off above  $T_1$  at the end of the latent heat determination. The temperature of the calorimeter dropped in a quasi-exponential manner with time until levelling off to a steady rate of drift some 10 or 15 min later. This slow approach to equilibrium, also observed by Ahlers,<sup>4</sup> always occurred in the two-solid mixture and made it difficult and tedious to get reliable heat capacity measurements in this region. To check our measurements and the consistency of the other data used in determining the latent heat, we also measured a sample (average molar volume  $V=21.13 \text{ cm}^3$ ) which did not intersect the pure bcc phase, but followed a path like that labeled "b" in Figs. 1 and 2. This sample contained

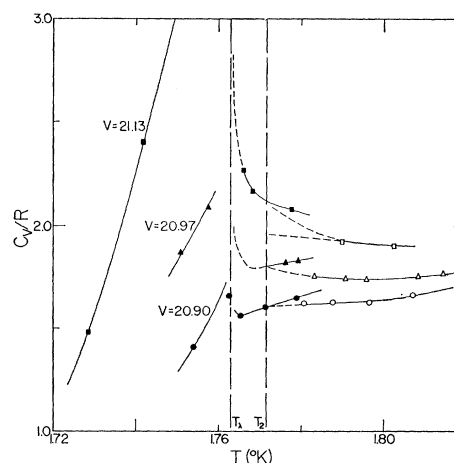


FIG. 3. The heat capacity of (liquid+solid)  $\text{He}^4$  at constant volumes in the neighborhood of  $T_1$  and the upper triple point  $T_2$ . The triangles refer to sample numbers 3 and 4 of Table III and the circles to sample number 7. The filled points refer to measurements on (bcc+liq) mixtures, including some superheated above  $T_2$ ; the open symbols refer to (hcp+liquid) mixtures. The heat capacity of both types of mixture at a given volume is approximately the same at  $T_2$ .

<sup>5</sup> D. O. Edwards and R. C. Pandorf, Phys. Rev. 140, A816 (1965).

liquid helium II both above and below  $T_1$ ; consequently, the thermal relaxation time was correspondingly lower, about 3 min. The latent heat  $L_2$  occurring at the upper triple point  $T_2$  and the heat capacity just below and just above  $T_2$  were also measured for several samples. The calorimeter contained liquid helium I both below and above the triple point (see a and b in Figs. 1 and 2) and the relaxation times were reasonably short.

It is a remarkable fact that the melting heat capacities measured just below and just above the triple points seem to be the same within experimental error. Figure 3 shows the measurements for three different molar volumes in the neighborhood of the melting  $\lambda$  point  $T_\lambda$  and the upper triple point  $T_2$ . The closed symbols represent measurements when the sample was partly bcc and partly liquid; the open symbols are for melting hcp. The closed symbols above  $T_2$  are for *superheated*, melting bcc. As the diagram shows, the results for melting hcp He<sup>4</sup> can all be extrapolated to  $T_2$  so as to intersect the curves for melting bcc, and the maximum difference in heat capacity at  $T_2$  between melting hcp and bcc samples at the same density is less than a few percent. The same fact is seen in Ahlers' measurements<sup>4</sup> for  $V = 20.940 \text{ cm}^3$ . At the lower triple point  $T_1$  following the melting curve (path b in Figs. 1 and 2), the difference in heat capacity is less than about 5%. At  $T_1$ , but following the transition line above  $T_1$  (path a), no definite conclusion could be reached because of the uncertainties introduced by the long relaxation time in the two-solid region. Some thermodynamic analysis of this apparent equality of the melting heat capacities at the triple points has been attempted, but without reaching a definite conclusion. It appears likely that the equality is not exact and that it can be justified only approximately.

The measured molar latent heats at the triple points, given in terms of entropies  $L_1/T_1$ ,  $L_2/T_2$ , are plotted as a function of the volume per mole of the sample  $V$  in Fig. 4. They can be understood by means of the following argument: Denote the three phases by the suffixes  $a, b, c$ , with the convention that phases  $a, b$ , are present below the triple point and  $a, c$ , above. Then the entropy

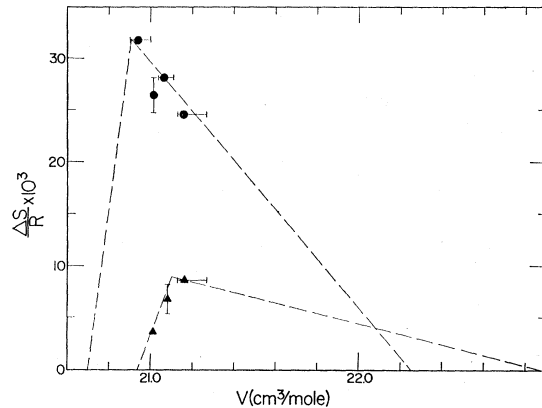


FIG. 4. The entropy change  $\Delta S/R = L/RT$  is shown at constant volume at the upper triple point  $T_2$  (circles) and at the lower triple point  $T_1$  (triangles) as a function of volume. The pairs of dashed lines are drawn to intersect the volume axis at the triple point volumes of the liquid and the hcp phases, measured by Grilly and Mills. At each triple point the pair of lines is drawn to intersect at the volume of the bcc phase since the maximum entropy changes will occur when  $V = V_{\text{bcc}}$ .

$S$  of the sample (all extensive quantities are molar) is given by

$$S = -\frac{dG}{dT} + V\frac{dp}{dT} = S_a + (V - V_a)\frac{dp}{dT}, \quad (1)$$

where  $G$  is the Gibbs function and where  $V_a$  and  $V$  are the volumes per mole of the phase  $a$  and of the sample as a whole. The total derivatives with respect to  $T$  are along the phase equilibrium line. The change in entropy at the triple point is therefore

$$\Delta S = \frac{L}{T} = (V - V_a) \left[ \left( \frac{dp}{dT} \right)_{ac} - \left( \frac{dp}{dT} \right)_{ab} \right]. \quad (2)$$

The measured latent heats are consistent with the linear dependence on  $V$  required by this equation, as is shown in Fig. 4, in which the volumes of the three phases at  $T_1$  and  $T_2$  are those determined by Grilly and Mills.<sup>3</sup> The maximum entropy changes,  $(\Delta S_1)_{\text{max}}$ ,  $(\Delta S_2)_{\text{max}}$ , which occur when  $V$  equals  $V_{\text{bcc}}$  are compared in Table I

TABLE I. The temperatures of the bcc-hcp-liquid triple points,  $T_1$  and  $T_2$ , and the upper  $\lambda$  point,  $T_\lambda$ . The maximum constant-volume entropy change at the triple points,  $(\Delta S_1)_{\text{max}}$  and  $(\Delta S_2)_{\text{max}}$ .

Source	$T_1$	$T_\lambda$	$T_2$	$10^3(\Delta S_1)_{\text{max}}/R$	$10^3(\Delta S_2)_{\text{max}}/R$
Vignos & Fairbank <sup>a</sup>	1.449 ± 0.003	1.765 ± 0.003	1.778 ± 0.003	...	...
Grilly & Mills <sup>b</sup>	1.437 ± 0.006	1.760 ± 0.001	1.760 ± 0.004	22	33
Ahlers <sup>c</sup>	1.464 ± 0.001	1.763 ± 0.003	1.773 ± 0.001	...	...
	-0.005				
Kierstead <sup>d</sup>	...	1.7633 ± 0.0001	1.7732 ± 0.0001	...	35.5 ± 2.0
Lounasmaa & Kaunisto <sup>e</sup>	...	1.762 ± 0.001	...	...	...
Present experiments	1.463 ± 0.002	1.763 ± 0.002	1.7715 ± 0.001	9 ± 1	32 ± 2

<sup>a</sup> Reference 1.

<sup>b</sup> Reference 3.

<sup>c</sup> Reference 4.

<sup>d</sup> Reference 6.

<sup>e</sup> O. V. Lounasmaa and L. Kaunisto, Ann. Acad. Sci. Fennicae, Ser. A, VI, No. 59 (1960).

with values calculated with Eq. (2) from  $PVT$  data. As the table shows, agreement at  $T_2$  between the present result, the one calculated from the slopes of the transition line and hcp melting curve (Grilly and Mills<sup>3</sup>), and the difference in melting curve slopes (Kierstead<sup>6</sup>) is excellent. At  $T_1$  the agreement is poor but our value of  $(\Delta S_1)_{\max}$  is quite consistent with  $(dp/dT)_{tr}$  obtained by Grilly and Mills at temperatures a little higher than  $T_1$ , and it appears that their value at  $T_1$  itself, which is anomalously high, is in error.

Table I also gives the triple-point temperatures  $T_1$  and  $T_2$ , and the temperature of the intersection of the  $\lambda$  line with the melting curve  $T_\lambda$ . In each case the result is the average of several determinations during different experiments with different densities, all of which are within the limits of error quoted. We are in very good agreement with the other authors except for Grilly and Mills,<sup>3</sup> and we have therefore followed Ahlers<sup>4</sup> and added a correction

$$\Delta T = 0.079 - 0.0375 T_{GM} \quad (3)$$

to Grilly and Mills' temperatures between  $T_1$  and  $T_2$  whenever we have had occasion to use their  $PVT$  data (as in Figs. 1, 2, and 4), so as to bring their triple points into agreement with Ahlers' and our own values.

### The Specific Heat

The heat capacities measured in the "pure" bcc phase are shown in Fig. 5, both directly and as the effective Debye temperature  $\Theta$ , for several different volumes. Temperature rises of about 0.006 deg were used in the measurements. The data were obtained after heating the sample into the (liquid+bcc) region and allowing it to

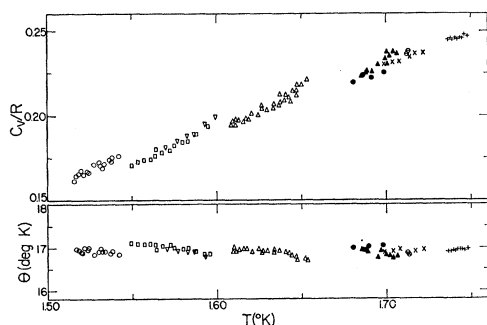


FIG. 5. Measurements of the specific heat at constant volume  $C_v$  of bcc He<sup>4</sup> for various molar volumes. The results are displayed both as  $C_v$  and as  $\Theta$ . The samples in the present measurements are described in Table III and are shown as:  $\circ$ , sample 1;  $\square$ , sample 2 ( $V=21.028$  cm<sup>3</sup>);  $\nabla$ , sample 3 ( $V=21.028$  cm<sup>3</sup>);  $\triangle$ , sample 5 ( $V=20.998$  cm<sup>3</sup>);  $\blacktriangle$ , sample 7 ( $V=20.943$  cm<sup>3</sup>);  $\ominus$ , sample 9 ( $V=20.927$  cm<sup>3</sup>); where the volumes quoted have been fitted to the melting line in the  $V$ - $T$  diagram of Fig. 2 using the measured values of the melting temperature. Ahlers' measurements (see Ref. 4) are for the following samples:  $\bullet$ ,  $V=20.955$  cm<sup>3</sup>;  $\times$ ,  $V=20.940$  cm<sup>3</sup>;  $+$ ,  $V=20.921$  cm<sup>3</sup>; where the volumes have also been fitted at the melting line.

<sup>6</sup> H. A. Kierstead, Phys. Rev. **138**, A1594 (1965); this issue, **144**, 166 (1966).

cool back into the bcc region of the phase diagram, or after holding the temperature steady in the bcc region for half an hour or so. Otherwise the heat capacity was higher and not reproducible and the heating curves showed small relaxation effects which were apparently due to small amounts of residual hcp phase which were able to remain for a considerable time. These were probably caused by pressure inhomogeneities: In particular, small regions of slightly higher pressure which were produced during the hcp-bcc transition and which slowly disappeared by the extrusion of the solid through the pores of the sintered copper calorimeter.<sup>5</sup> When all traces of the residual hcp phase had been removed, it was possible to supercool the bcc solid about 10 mdeg or so below the lower phase boundary, and to measure the temperature of the phase boundary with some precision (see Fig. 6). Unfortunately, we were never able

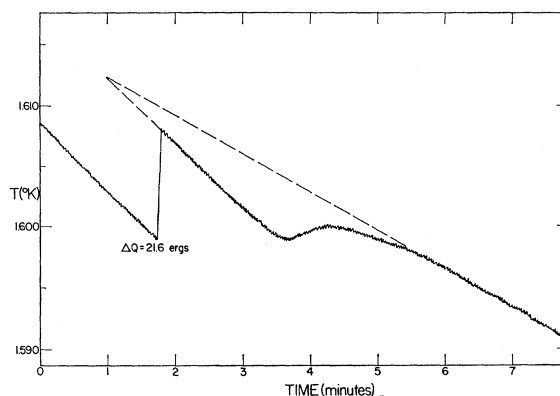


FIG. 6. Temperature of the calorimeter versus time taken from a recorder tracing. At  $t=0$  the sample (number 5, Table III) is in the (supercooled) bcc state and is cooling by heat loss through a superconducting indium thermal switch. At  $t=1.8$  min the heat capacity is determined in this supercooled state. Just after  $t=3$  min, hcp solid begins to appear and the calorimeter is heated slightly by the latent heat of transformation. At  $t=5.5$  min, the drift rate is steady once more and hcp and bcc are judged to be very near to equilibrium. Assuming that the rate of heat loss is constant over this small range of temperature, extrapolation of the curves gives the bcc-hcp boundary in the absence of supercooling to be  $1.612 \pm 0.001$  °K.

to superheat the bcc solid above its melting point, even after half an hour of annealing. Moreover, the increase in specific heat at melting was not completely sharp but showed a small "tail" up to 20 mdeg before the main discontinuity, although the data in this region were quite reproducible both on cooling and heating. These phenomena indicate that freezing probably left some small regions of slightly lower than normal pressure or density which we were unable to remove by annealing.

Figure 5 also shows the data of Ahlers<sup>4</sup> obtained at the high-temperature end of the bcc phase. Both his data and ours lie rather close to one curve and can be represented to within about 3% of  $C_v$  by a Debye formula with  $\Theta=16.95$  °K for all densities. This behavior is similar to that of the thermal conductivity

measured by Berman and Rogers<sup>7</sup> which, when plotted against temperature, also lies on one curve irrespective of density. Ahlers has interpreted his specific-heat results as indicating that the bcc phase has some anomalous properties in the high density part of the phase diagram, in agreement with a theory of Goldstein<sup>8</sup> which predicts anomalous thermal properties of the solid near the intersection of the  $\lambda$  line with the melting curve. Ahlers bases his conclusions partly on the fact that, in his experiments, the specific heat appears to decrease with increasing molar volume at fixed temperature (see Fig. 5). In our experiments the tail or premelting effect in the heat capacity makes the temperature and volume dependence of  $C_v$  or  $\Theta$  difficult to determine, but  $C_v$  appears to *increase* with increasing  $V$ , which is the behavior observed in bcc He<sup>3</sup> and in hcp He<sup>3</sup> and He<sup>4</sup>.

### The Entropy

The specific-heat measurements on some samples (3, 6, 8, and 9 in Table III) extend from the hcp phase past the lower triple point  $T_1$  and across the two-phase hcp+ bcc region. From these measurements we have been able to obtain the entropy of the bcc phase of He<sup>4</sup> by integrating  $C_v/T$  and adding the appropriate entropy change at  $T_1$ . The results for the entropy at the transition curve are given in Fig. 7 as the square symbols. The experimental error indicated in the graph is approximate and is based on the estimated 10% accuracy of the heat capacity measurements in the two-phase region where the thermal relaxation time is long. The figure also gives a value of  $S$  at the lower triple point  $T_1$  (the closed circle). This was obtained by adding  $(\Delta S_1)_{\max}$  (Fig. 4) to the entropy of the mixture of hcp He<sup>4</sup> and liquid He<sup>4</sup> which transforms to bcc He<sup>4</sup> at  $T_1$ . The entropy of the (hcp+liquid) mixture was determined from the data on hcp He<sup>4</sup> given in our previous paper,<sup>5</sup> the entropy of freezing liquid helium at  $T_1$  given by van den Meijdenberg, Taconis and Ouboter,<sup>9</sup> plus the molar volume data given by Grilly and Mills.<sup>3</sup> The inverted open triangles in Fig. 7 represent values calculated from the formula  $S_{\text{bcc}} = S_{\text{hcp}} + \Delta S_{\text{tr}} = S_{\text{hcp}} + \Delta V_{\text{tr}}(dp/dT)_{\text{tr}}$ , where  $(dp/dT)_{\text{tr}}$  and  $\Delta V_{\text{tr}}$  were taken from Grilly and Mills. The uncertainty in these points is mainly in the value of  $\Delta S_{\text{tr}}$  which was estimated to be  $\pm 10\%$  by Grilly and Mills. The inverted, filled triangle at  $T_2$  was obtained in the same manner but using the new measurements of Kierstead<sup>6</sup> for  $(dp/dT)_{\text{tr}}$ . The open circles in the figure were calculated from  $S_{\text{bcc}} = S_{\text{liq}} - \Delta S_m - \Delta S'$ , where  $\Delta S_m = \Delta V_m(dp/dT)_m$  is from Grilly and Mills,  $S_{\text{liq}}$  is from the data of van den Meijdenberg *et al.*,<sup>9</sup> and  $\Delta S'$  is a small correction for the difference between the entropy of the bcc phase at melting and at the transition line.  $\Delta S'$  was estimated from the present heat-capacity data

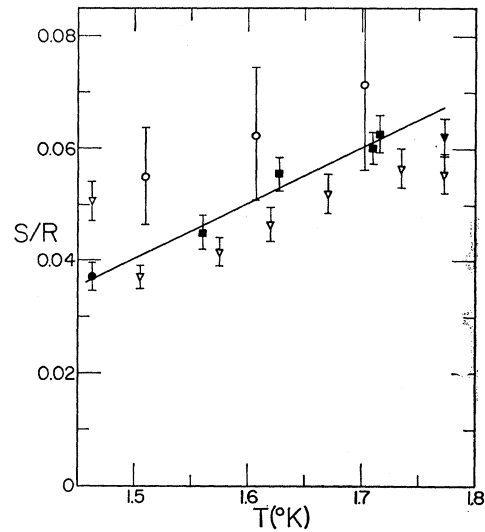


Fig. 7. The entropy of bcc He<sup>4</sup> at the hcp-bcc transition line. The solid squares show the entropy by integration of  $C_v/T$  using the present  $C_v$  measurements in the hcp, (hcp+liq) and (hcp+bcc) regions together with the value of the latent heat at  $T_1$ . The solid circle gives the entropy at the lower triple point determined from the maximum value of the entropy change at  $T_1$ ,  $(\Delta S_1)_{\max}$ , the entropy of the liquid at the lower triple point from van den Meijdenberg *et al.* (see Ref. 9) and the entropy of hcp He<sup>4</sup> at  $T_1$  (see Ref. 5). The open triangles show  $S_{\text{bcc}} = S_{\text{hcp}} + \Delta V_{\text{tr}} \times (dp/dT)_{\text{tr}}$  using  $\Delta V_{\text{tr}}$  and  $(dp/dT)_{\text{tr}}$  from Grilly and Mills (see Ref. 3) and  $S_{\text{hcp}}$  from Ref. 5; the closed triangle gives the same, but using  $(dp/dT)_{\text{tr}}$  from Kierstead (see Ref. 6). The open circles show  $S_{\text{bcc}} = S_{\text{liq}} - \Delta V_m(dp/dT)_m - \Delta S'$  using  $S_{\text{liq}}$  from van den Meijdenberg *et al.* and  $\Delta V_m(dp/dT)_m$  from Grilly and Mills. ( $\Delta S'$  is a small correction for the difference in entropy below on the melting line and the transition line.) The straight line has been drawn through our values of the entropy.

and amounts to 4% of  $S_{\text{bcc}}$  at most. As the figure shows, all the values of  $S_{\text{bcc}}$  are in good agreement, within the expected errors, with the smoothed curve through the present data.

The entropy results together with the specific heat have been used to give some information about the possible temperature dependence of the Debye theta of bcc He<sup>4</sup> in the temperature range down to 0°K. In this region, of course, the hcp phase and the liquid are the thermodynamic equilibrium states but, in principle, the bcc solid could exist in a metastable "supercooled" state. The hypothetical temperature dependence of  $\Theta$  in this region has been studied by plotting the ratio of the entropy to the specific heat,  $S/C_v$ , versus a function of the specific heat,  $T/\Theta$ , which is approximately proportional to the temperature. The graphs for hcp He<sup>4</sup>, from our previous paper,<sup>5</sup> for bcc He<sup>4</sup>, and some results for bcc and hcp He<sup>3</sup> are all given in Fig. 8. The specific-heat measurements on the He<sup>3</sup> phases were made by the same technique as in the present work and will be described in a later paper. The He<sup>3</sup> entropies were calculated by direct integration of the specific heat for  $T/\Theta \geq 0.025$ . For  $T/\Theta < 0.025$ , the Debye entropy was assumed, thus ignoring spin entropy and effects due to He<sup>4</sup> impurity. Figure 8 also shows graphs of  $\Theta/\Theta_0$

<sup>7</sup> R. Berman and S. J. Rogers, Phys. Letters **9**, 115 (1964).

<sup>8</sup> L. Goldstein, Phys. Rev. **122**, 726 (1961).

<sup>9</sup> C. J. N. van den Meijdenberg, K. W. Taconis, and R. de Bruyn Ouboter, Physica **27**, 197 (1961).

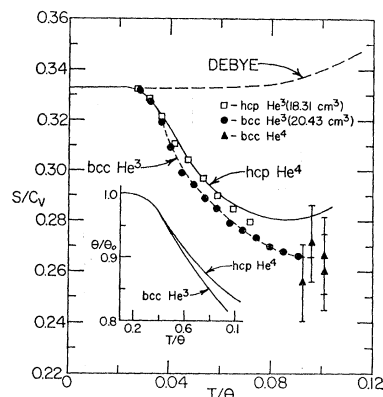


FIG. 8.  $S/C_v$  versus  $T/\Theta$  for the various low-pressure helium structures; the dashed line gives the curve for the Debye model. The insert to the figure shows  $\Theta/\Theta_0$  versus  $T/\Theta$  for hcp  $\text{He}^4$  and bcc  $\text{He}^3$  (hcp  $\text{He}^3$  is nearly the same as hcp  $\text{He}^4$  and is not shown).

versus  $T/\Theta$  for the different forms of solid helium ( $\Theta_0$  is the value of  $\Theta$  at  $0^\circ\text{K}$ ). It may be seen that the entropy-specific-heat curves reflect the dependence of  $\Theta$  on  $T/\Theta$  very well. The points for bcc  $\text{He}^4$  lie very close to the curves for the other forms of solid helium, which all have very similar  $\Theta/\Theta_0$ - $T/\Theta$  curves, which suggests that the specific heat and Debye  $\Theta$  of "supercooled" bcc  $\text{He}^4$  would have approximately the same temperature dependence as the other forms of solid helium. The agreement is closest with the  $S/C_v$  curve for bcc  $\text{He}^3$  of approximately the same molar volume ( $V=20.43\text{ cm}^3$ ), so that we have used this curve to extrapolate our  $\Theta$  values for bcc  $\text{He}^4$  to  $0^\circ\text{K}$ . The results of this calculation are given in Table II.

The calculated values of  $\Theta_0$  for "supercooled" bcc  $\text{He}^4$  have approximately the same dependence on  $V$  as the other solid helium allotropes in this volume range. These have a Gruneisen constant  $\gamma=2.6$ , so that  $\Theta_0 \propto V^{-2.6}$ . It is interesting to compare the magnitudes of  $\Theta_0$  in the four low-pressure forms of solid helium: The ratio  $\Theta_0(\text{He}^3)/\Theta_0(\text{He}^4)$  at a given volume is 1.17 for the hcp structure, much closer to the "classical" harmonic value  $\sqrt{4/3}=1.155$  than that for the bcc structure which is 1.23.

### The Phase Diagram

We have already described the method of measuring the temperature of the (hcp+bcc)-(bcc) phase boundary, above and in the caption of Fig. 6. The melting temperature of the bcc phase was more difficult to determine because of the tail or premelting before the main discontinuity in heat capacity and because of the size of the temperature intervals used in measuring the heat capacity. The melting point appeared as a

TABLE II. The Debye  $\Theta$  of bcc  $\text{He}^4$  extrapolated to  $0^\circ\text{K}$ . Units are  $^\circ\text{K}$ . The error is  $\pm 0.4^\circ\text{K}$ .

Molar volume $V$ ( $\text{cm}^3$ )	20.927	20.932	20.988	21.028
$\Theta_0$	21.2	21.1	20.95	20.8

very steep rise in heat capacity, less than a few millidegrees wide, giving values for the melting temperatures to about  $\pm 0.003^\circ\text{K}$ . In order to make a meaningful comparison of these results with those of previous workers, we have fitted our melting points to the smoothed melting  $V$ - $T$  curve for bcc  $\text{He}^4$  obtained by Grilly and Mills<sup>3</sup> (open circles in Fig. 2), corrected using the formula suggested by Ahlers,<sup>4</sup> [Eq. (3)]. This procedure was used to determine the molar volume by Ahlers, whose points are shown as open triangles. As Fig. 2 shows, with the volumes normalized in this way the data from all three sources are in good agreement.

As explained in the description of experimental technique in our first paper,<sup>5</sup> we have also measured the molar volume of our samples directly by measurements on the gas at room temperature, and less directly, by determining the freezing point of the hcp phase and then using Grilly and Mills' melting curve data.<sup>3,10</sup> These values which are given, when available, in Table III are in fair agreement with each other and the values used in Fig. 2, although the discrepancies are slightly larger than 0.2% in  $V$ , the expected experimental accuracy.

### The Compressibility

Since bcc  $\text{He}^4$  exists over only a narrow range of density and temperature, one would expect that the compressibility  $\kappa = -(1/V)(\partial V/\partial p)_T$  is fairly constant over the whole bcc region of the phase diagram. Approximate values of  $\kappa$  can be calculated in a number of ways from the available experimental data:

(i) From the pressure, volume, and temperature ( $PVT$ ) along the phase boundaries, one can calculate the *average* isothermal compressibility across the phase. In Fig. 10 the curve marked  $PVT$  was calculated in this way by Ahlers.<sup>4</sup>

(ii) From the discontinuous change in heat capacity,  $\Delta C_v$ , at the boundaries of the bcc phase using the thermodynamic equation<sup>11,12</sup>

$$\kappa = (T/V\Delta C_v)(dV/dT)^2, \quad (4)$$

where  $(dV/dT)$  is the slope of the phase boundary in the  $V$ - $T$  diagram (Fig. 2). The  $\Delta C_v$  data for both boundaries of the bcc phase have been collected in Fig. 9 which shows that Ahlers'<sup>4</sup> measurements and the present ones are in fairly good agreement. The compressibilities calculated with Eq. (4) from the smoothed curves for  $\Delta C_v$  and from  $dV/dT$  obtained from Grilly and Mills'<sup>3</sup> measurements are shown in Fig. 10 as the curves  $A_t$  and  $A_m$ . Here  $A_t$  refers to the bcc compressibility along the hcp-bcc transition line;  $A_m$  refers to the melting line. These curves are similar to the ones published by Ahlers but extend to lower temperatures.

(iii) From the variation of  $V$  with pressure along the

<sup>10</sup> E. R. Grilly and R. L. Mills, *Ann. Phys. (N. Y.)* **8**, 1 (1959).

<sup>11</sup> L. Goldstein, *J. Wash. Acad. Sci.* **40**, 97 (1950).

<sup>12</sup> O. V. Lounasmaa, *J. Chem. Phys.* **33**, 443 (1960).

TABLE III. The samples of solid He<sup>4</sup>. The table gives the initial, or freezing pressure,  $P_f$ ; the directly measured volume per mole of the sample,  $V_{\text{meas}}$ ; the observed values of the bcc melting temperature,  $T_{\text{melt}}$ ; the temperature at the hcp-bcc transition line,  $T_{\text{tr}}$ ; and the freezing temperature,  $T_f$ . The volumes in parentheses below the values of  $P_f$ ,  $T_{\text{melt}}$ ,  $T_{\text{tr}}$ , and  $T_f$  have been calculated from them using the  $PVT$  data of Grilly and Mills, corrected where necessary with Eq. (3).

Sample number	$P_f$ (atm) $\pm 0.02$ atm	$V_{\text{meas}}$ (cm <sup>3</sup> ) $\pm 0.04$ cm <sup>3</sup>	$T_{\text{melt}}$ (°K) $\pm 0.003$	$T_{\text{tr}}$ (°K) $\pm 0.002$	$T_f$ (°K) $\pm 0.002$
1	46.0 (21.08)	...	...	...	...
2	46.2 (21.07)	...	1.632 (21.028)	1.561	...
3	46.3 (21.06)	21.11	1.632 (21.028)	...	2.237 (21.11)
4	46.3 (21.06)	20.97	1.632 (21.028)	...	2.242 (21.10)
5	47.3 (21.01)	21.04	1.674 (20.998)	1.612	2.260 (21.06)
6	47.3 (21.01)	...	1.685 (20.988)	1.627 $\pm$ 1	2.284 (21.01)
7	48.6 (20.94)	20.90	1.730 (20.943)	1.691	2.291 (21.00)
8 <sup>a</sup>	48.6 (20.94)	...	...	1.708 (20.932)	...
9	48.7 (20.93)	20.86	1.746 (20.927)	1.712 $\pm$ 3	...

<sup>a</sup> This sample crossed the hcp-(hcp+bcc) boundary at  $1.482 \pm 0.003$ °K.

phase boundaries, using the Gruneisen equation for the isobaric expansion coefficient,  $\alpha = (1/V)(\partial V/\partial T)_p = \gamma \kappa C_v/V$ , to correct for the change in  $V$  caused by thermal expansion. This method results in the equation:

$$\kappa = (dV/dT)/[\gamma C_v - V(dp/dT)], \quad (5)$$

where  $\gamma$  is the Gruneisen constant which we have assumed to be approximately 2.6 (see the discussion above on the entropy of bcc He<sup>4</sup>). The values of  $\kappa$  calculated from Eq. (5) for bcc He<sup>4</sup> along the melting curve are shown in Fig. 10 by the curve  $B_m$ .

(iv) The quantity  $(dV/dT)$  along the phase boundaries can be eliminated from the calculation of  $\kappa$  by combining Eqs. (4) and (5):

$$\kappa = V \Delta C_v / T [\gamma C_v - V(dp/dT)]^2. \quad (6)$$

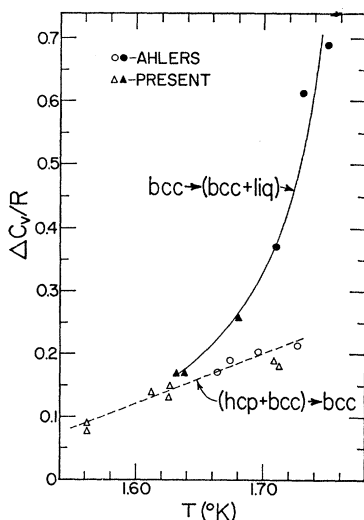


FIG. 9. The change in heat capacity at constant volume  $\Delta C_v/R$  at the bcc phase boundaries as a function of temperature. The open symbols refer to the hcp-bcc transition line, the closed symbols to the melting line.

This method gives the closed circles for the compressibility on the transition line and the closed squares for the melting line. The approximate experimental error indicated on these points has been estimated from the uncertainty in  $\Delta C_v$  and  $\gamma$ . (The term in  $\gamma$  has only a small effect on the results for  $\kappa$ .) The average value of these points is  $\kappa = (3.8 \pm 0.2) \times 10^{-3}$  atm<sup>-1</sup>.

Curve C in Fig. 10 represents some unpublished, direct measurements<sup>13</sup> of  $\kappa$  by Grilly. These extend from  $\kappa = 3.4 \times 10^{-3}$  atm<sup>-1</sup> at 1.48°K to  $4.2 \times 10^{-3}$  atm<sup>-1</sup> at 1.74°K with a scatter of about 5% in  $\kappa$ . Another direct

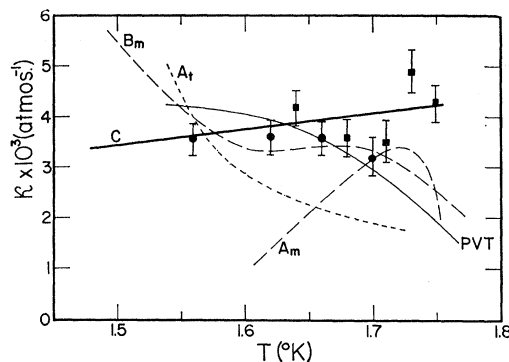


FIG. 10. The isothermal compressibility  $\kappa$  of bcc He<sup>4</sup> as a function of temperature. The points were calculated from Eq. (6). The squares refer to the melting line and the circles are for the hcp-bcc transition line. The line C represents some unpublished, direct measurements of  $\kappa$  along the melting line by Grilly (see Ref. 13). The other curves are explained in the text.

<sup>13</sup> E. R. Grilly (unpublished). The authors are grateful to Dr. Grilly for this data in advance of publication.

measurement, by Kidder<sup>14</sup> and not shown in Fig. 10, gives  $(4.7 \pm 0.3) \times 10^{-3} \text{ atm}^{-1}$  between 1.55 and 1.7°K.

The values of  $\kappa$  from method (iv), i.e., from Eq. (6), are self-consistent within the experimental error in that the results for the transition line are the same as those along the melting line and are independent of temperature. They also agree with the preliminary, direct measurements of Grilly. The wide variations in  $\kappa$ , which are given by the first three methods described above, are probably due to small inaccuracies in the volume-temperature data which are not sufficiently accurate to give derived quantities like  $dV/dT$ .

### The Expansion Coefficient

The isobaric expansion coefficient of bcc He<sup>4</sup> can, like the compressibility, also be estimated in a number of ways from the experimental data which are presently available. The methods are similar to the ones for the compressibility discussed above. For instance, the expansion coefficient can be obtained as an average across the bcc phase using Figs. 1 and 2. Another way is by using values of  $dV/dT$  and  $\Delta C_v$  as in method (ii) for the compressibility. Such calculations, which have been discussed by Ahlers,<sup>4</sup> give values of  $\alpha$  which vary widely with temperature and volume and in some cases give negative values of  $\alpha$ . The discussion of the compressibility above has shown that the variation of  $V$  with  $T$  is not known sufficiently accurately at present for such calculations to be at all reliable. Moreover, Kidder<sup>14</sup> has shown by direct measurement that the isobaric expansion coefficient is positive and less than  $10^{-2} \text{ deg}^{-1}$  between 1.57 and 1.72°K. Self-consistent values of  $\alpha$  can be obtained by eliminating  $dV/dT$  from the input data. Using the equation  $dV/dT = V[\alpha - \kappa(d\rho/dT)]$  with Eq. (4), one obtains

$$\alpha = \kappa(d\rho/dT) + (\kappa\Delta C_v/VT)^{1/2}. \quad (7)$$

The result of applying Eq. (7) to the melting curve is shown as the squares in Fig. 11, while the results along the transition line are shown as circles. These two sets of values are quite consistent with each other and also

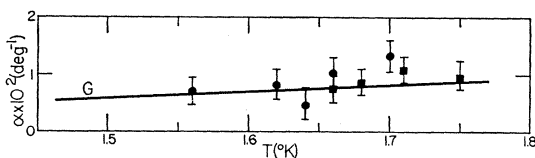


FIG. 11. The expansion coefficient  $\alpha$  of bcc He<sup>4</sup> as a function of temperature. The continuous line G is calculated from the Gruneisen equation,  $\alpha = (\gamma\kappa C_v/V)$ , assuming  $\gamma = 2.6$ . The points are calculated from Eq. (7),  $\alpha = \kappa(d\rho/dT) + (\kappa\Delta C_v/VT)^{1/2}$ . The circles are for the hcp-bcc transition, the squares for the melting line. The compressibility  $\kappa$  was estimated from Fig. 10,  $V$  and  $(d\rho/dT)$  from Grilly and Mills,  $C_v$  and  $\Delta C_v$  from Ahlers' and the present work.

<sup>14</sup> J. N. Kidder, in *Proceedings of the Eighth International Conference on Low Temperature Physics*, edited by R. O. Davies (Butterworths Scientific Publications, Inc., Washington, 1963), p. 419.

with those from a completely different method, curve G, which was calculated from the Gruneisen equation,  $\alpha = \gamma\kappa C_v/V$ , using  $\gamma = 2.6$ .

### Elastic Anisotropy

The elastic properties of bcc He<sup>4</sup> can be studied with the help of the velocity of longitudinal sound, measured by Vignos and Fairbank,<sup>1,15</sup> and the recent measurements of the velocity of shear waves by Lipschultz and Lee.<sup>16</sup> The sound measurements are consistent with the values of the compressibility in Fig. 10 if we assume the samples studied in the sound experiments were isotropic, since the equation,  $v_t^2 = (1/\kappa\rho) + (4v_l^2/3)$ , appropriate to an isotropic (or polycrystalline) solid gives a value of  $3.8 \times 10^{-3} \text{ atm}^{-1}$ , in excellent agreement with the present data. (It is estimated that the difference between the adiabatic and isothermal compressibilities is about 2%.) If the bcc He<sup>4</sup> crystal were itself isotropic, the value of the Debye theta at 0°K,  $\Theta_0$ , could be calculated from the equation

$$\Theta_0 = \frac{\hbar}{k} \left( \frac{6\pi^2 N_0}{V} \right)^{1/3} \left( \frac{2}{3v_t^3} + \frac{1}{3v_l^3} \right)^{-1/3}$$

if  $v_t$  and  $v_l$  are the sound velocities at 0°K. This equation gives  $\Theta_0 = 35^\circ\text{K}$ , which is very high compared to the values of  $\Theta_0$  in Table II ( $\sim 21^\circ\text{K}$ ) and the values of  $\Theta$  given in Fig. 5 ( $\sim 17^\circ\text{K}$ ). This result demonstrates that bcc He<sup>4</sup> is elastically highly anisotropic. The scatter in the velocity of sound measurements from one specimen to another was quite small,<sup>1,15,16</sup> so that we can deduce that all the sound measurements were made on polycrystalline specimens containing a large number of crystals.

Recently, Nosanow and Werthamer<sup>17</sup> have developed a theory of the vibrational modes of both bcc and hcp solid helium and have given values for the principal sound velocities for He<sup>4</sup> and He<sup>3</sup> at various densities. Their theory shows that both structures should be very anisotropic. We have compared the present results with the theory by calculating the elastic constants  $c_{11}$ ,  $c_{12}$ , and  $c_{44}$  from the theoretical sound velocities. From these elastic constants we have obtained  $\kappa$ , the compressibility at 0°K, and  $\Theta_0$ , the Debye theta at 0°K. For  $v = 21.00 \text{ cm}^3$ , the theoretical value of  $\kappa$  is about  $3.4 \times 10^{-3} \text{ atm}^{-1}$ , in good agreement with experiment; the theoretical

<sup>15</sup> J. H. Vignos and H. A. Fairbank, in *Proceedings of the Eighth International Conference on Low Temperature Physics*, edited by R. O. Davies (Butterworth's Scientific Publications, Inc., Washington, 1963), p. 31.

<sup>16</sup> R. P. Lipschultz and D. M. Lee, *Phys. Rev. Letters* **14**, 1017 (1965).

<sup>17</sup> L. H. Nosanow and N. R. Werthamer, *Phys. Rev. Letters* **15**, 618 (1965). Note that the degeneracies of the transverse modes in Table I and Fig. 2 of this paper are incorrectly assigned. Table I should read for the transverse [110] mode: 174, 343 m/sec for  $V = 19.88 \text{ cm}^3$ , and 152, 335 m/sec for  $V = 21.63 \text{ cm}^3$ ; for the transverse [100] mode, 343(2) and 335(2) m/sec for the same two volumes. We are grateful to Dr. L. H. Nosanow for a discussion of this point.



value of  $\Theta_0$ , obtained by the "semi-analytic" method described by de Launay,<sup>18</sup> is 24.5°K, again in fairly good agreement with the values in Table II.

### III. CONCLUSION

In summary, our data indicate that bcc He<sup>4</sup> is probably not much different from the other forms of solid helium. This is based upon the following results discussed in detail above:

(a) The compressibility  $\kappa$  and the expansion coefficient  $\alpha$  are well behaved. The expansion coefficient is positive and agrees with the Gruneisen equation with a Gruneisen constant  $\gamma=2.6$ , which is the value found for the other low-pressure forms of solid helium and which is not inconsistent with the variation of the Debye  $\Theta$  with

<sup>18</sup> J. de Launay, in *Solid State Physics*, edited by F. Seitz and D. Turnbull (Academic Press Inc., New York, 1956), Vol. II, p. 285.

volume in the present measurements. As was illustrated in Fig. 10, the  $V$ - $T$  data available at present are not precise enough to use  $dV/dT$  to obtain either  $\kappa$  or  $\alpha$ , so that earlier calculations which gave negative values of  $\alpha$  are unreliable.

(b) The entropy of bcc He<sup>4</sup> when plotted as  $S/C_v$  versus  $T/\Theta$  (Fig. 8) is found to be consistent with the values for the other low-pressure, crystalline forms of He<sup>4</sup> and He<sup>3</sup>, indicating that the temperature dependence of  $\Theta$  and the lattice spectra are very similar.

### ACKNOWLEDGMENTS

It is a pleasure to thank Dr. Robert Frost, Edward Ifft, and Peter Seligmann for their help in making the measurements, Professor J. G. Daunt for his support and encouragement, and Robert Kindler, W. E. Baker, and Larry Wilkes for their technical assistance.

## Equations of Motion in Nonequilibrium Statistical Mechanics\*†

BALDWIN ROBERTSON‡

*Laboratory of Atomic and Solid State Physics, Physics Department, Cornell University, Ithaca, New York*

(Received 1 July 1965; revised manuscript received 8 November 1965)

Exact equations of motion for the space- and time-dependent thermodynamic coordinates of a many-body system are derived directly from the Liouville equation. This is done by defining a generalized canonical density operator depending only upon present values of the thermodynamic coordinates. This operator is used no matter how far the system is from equilibrium. An explicit expression for the entropy of a system possibly not in equilibrium is given in terms of this operator. The equation of motion for the operator is derived, and the coupled, nonlinear, integrodifferential equations of motion for the thermodynamic coordinates follow immediately.

### INTRODUCTION

EQUATIONS of motion for the thermodynamic coordinates of a many-body system have been remarkably successful in describing the results of nonequilibrium experiments. The equations of hydrodynamics, London's equations for superconductors, and Bloch's equations for nuclear magnetism are well-known examples. Originally, these equations were not derived from microscopic considerations, but were obtained by more or less qualitative physical reasoning and contained adjustable parameters whose values were determined empirically. Since the assumptions made in order to obtain these phenomenological equations limited their applicability, it would be desirable to generalize these equations and thus extend their usefulness.

Unfortunately, it is not easy to just guess phenomenological improvements for these equations by using qualitative physical reasoning alone. Furthermore, it would be desirable to be able to calculate the values of the parameters appearing in the equations. Thus we are led to derive these equations from the Liouville equation and thereby obtain formal expressions for the parameters.

Once we have derived the equations, they may be solved as if they were classical equations, and in this manner many problems in nonequilibrium statistical mechanics can be solved. This equation of motion approach yields more general results than the perturbation-theory approach used in the linear theory of irreversible processes. In particular, we will be able to describe systems that may be arbitrarily far from equilibrium, and this is not possible with the linear theory.

The characteristic feature of our method is that no matter how far the system is from equilibrium we use a generalized canonical density operator  $\sigma(t)$  that is a

\* Supported in part by the Advanced Research Projects Agency.

† Based on a dissertation submitted to Stanford University, 1964.

‡ National Science Foundation Predoctoral Fellow, 1956-1959.